Observation of ballistic transport in the upper subband of a two-dimensional electron system

J. P. Lu and M. Shayegan
Department of Electrical Engineering, Princeton University, Princeton, New Jersey 08544
(Received 20 October 1995)

We report a specially designed transverse magnetic focusing experiment on a two-dimensional electron system confined to a square quantum well with two electric subbands occupied. The reflecting barrier of a usual magnetic focusing device is replaced by a surface-gate-induced, tunable potential barrier that allows us to selectively reflect and magnetically focus the upper subband electrons while the lower subband electrons pass over the barrier and are not focused. We observe the focusing of the upper subband electrons. The weakness of the focusing signal for the upper subband ballistic electrons suggests that they have a surprisingly short ballistic mean free path compared to the lower subband electrons.

The low-disorder two-dimensional electron system (2DES) confined to a wide quantum well and occupying two electronic subbands is of considerable interest as it exhibits new phenomena arising from the electron-electron interactions.[1] The ballistic transport of electrons in such systems, however, has remained unexplored. More generally, the details of the ballistic electron transport in a two-subband 2DES confined to a potential well of *any* shape is unknown. In order to explain an anomalous feature in their magnetic focusing data on a $GaAs/Al_xGa_{1-x}As$ 2DES, Laikhtman *et al.*[2] invoked the injection of electrons into the upper subband of the 2DES and suggested that these electrons possess an expectedly *long* mean free path (MFP). Later data,[3,4] however, have revealed a very similar feature in 2DES's where the upper subband is clearly not occupied; these data in fact strongly suggest that this anomalous feature is not related to the upper subband electrons (USE's) and that it can be understood in terms of the lower subband electrons (LSE's) at higher injection energy. Therefore, the demonstration of the ballistic transport in the upper subband of a 2DES has remained an experimental challenge. Here we provide such a demonstration. Our data suggest that the ballistic MFP for the USE's is in fact surprisingly *short* compared to the LSE's.

One of the most direct techniques for studying the upper subband ballistic electrons is a transverse magnetic focusing (TMF) experiment,[5,6] schematically shown in Fig. 1. In a standard TMF experiment [Fig. 1(a)], a beam of ballistic electrons emitted by passing a current through a narrow constriction (injector) is deflected by a perpendicular magnetic field B and impinges on a second opening (collector). Along the distance, L, between the injector and collector openings is a reflecting barrier, realized by depleting the 2DES in this region. The collector voltage exhibits periodic maxima as a function of B, corresponding to the matching of the length L with integral multiples of the electron cyclotron orbit diameter, with the period $\Delta B=(2\hbar/e)(k_f/L)$, where k_f is the electron Fermi wave vector. The application of the TMF to studies of the ballistic transport in single-subband 2DES's has been reported and is well understood.[6,7]

In a standard TMF experiment on a double-subband system, since k_f for the LSE's and USE's is different, one may expect two sets of focusing peaks, each with periodicity corresponding to either the LSE or USE trajectories, as shown in Fig. 1(b). We have done extensive TMF measurement with the geometry of Fig. 1(b) on a number of high-quality two-subband 2DES's confined to wide GaAs quantum wells but have not been able to observe the ballistic transport of the USE's. An example of our data is shown in Fig. 1(c) for a TFM device with $L=6$ μm. The trace in Fig. 1(c) and its Fourier power spectrum, shown in the inset, reveal the presence of oscillations at only one frequency which closely matches the frequency expected for the focusing of the LSE's. The focusing signal of the USE is conspicuously absent.

One possible explanation for the absence of the USE focusing signal is that this signal is particularly weak and is masked by the strong signal from the LSE's. In order to study the ballistic USE's, therefore, we made a special TMF device to eliminate the focusing signal of the LSE's while preserving that of the USE's. In this device, which is illustrated in Fig. 2, the fixed, fully reflecting barrier of the standard TMF experiment is replaced by a barrier whose height can be adjusted by applying a bias, V_g, between a surface metal gate and the 2DES. For $V_g\approx 0$, the potential barrier seen by the 2DES has negligible height and is therefore transparent to the ballistic electrons of both subbands [Fig. 2(a)]. Only two focusing peaks corresponding to the cyclotron orbit diameters of the electrons in the two subbands matching L should be observable. When $V_g \ll 0$ [Fig. 2(c)], on the other hand, the barrier reflects electrons in both subbands; this corresponds to the standard TMF experiment. Figure 2(b) illustrates the intermediate $V_g<0$ case which is of particular interest here: the USE's are reflected and should exhibit TMF while LSE's can pass over the barrier and should not reach the collector except of course at B where their orbit diameter equals L. Here we report the successful implementation of this ''filtering'' technique to observe the TMF of USE's.

Our sample was grown by molecular-beam epitaxy and contains a 2DES which is confined to a 450-Å-wide GaAs quantum well located 1500 Å underneath the surface. The quantum well is flanked on both sides by 650-Å-wide undoped $Al_{0.35}Ga_{0.65}As$ spacer and Si dopant layers. Surface gates are formed by electron-beam lithography followed by Cr/Au deposition and lift-off process. Figure 2(d) shows a scanning electron micrograph of the device. The center, Γ-shaped gate, which produces the tunable barrier is 2000 Å wide. Two pairs of split gates which can be biased separately are also deposited on each side of the center gate and are

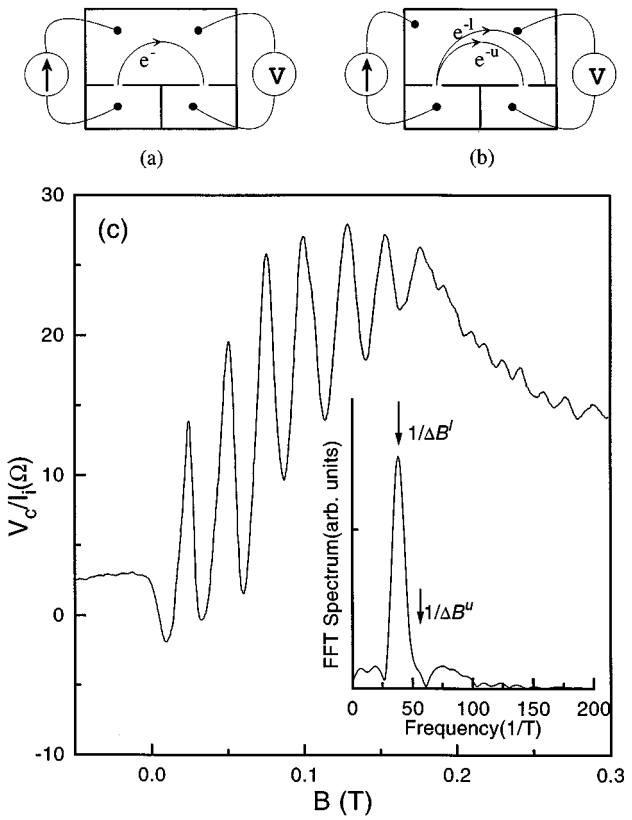

FIG. 1. (a) Schematic diagram for a standard TMF experiment. (b) Schematic diagram depicts a standard TMF device applied to a two-subband system. The half circles represent the different electron trajectories, at a given B, corresponding to electrons in the two subbands. (c) Measured TMF spectrum (collector voltage normalized by the injector current vs B) in a standard focusing device on a two-subband sample. The inset shows the Fourier transform of these data; the arrows indicate the expected frequencies of the focusing spectra for the USE's and LSE's, marked by $1/\Delta B^u$ and $1/\Delta B^l$, respectively.

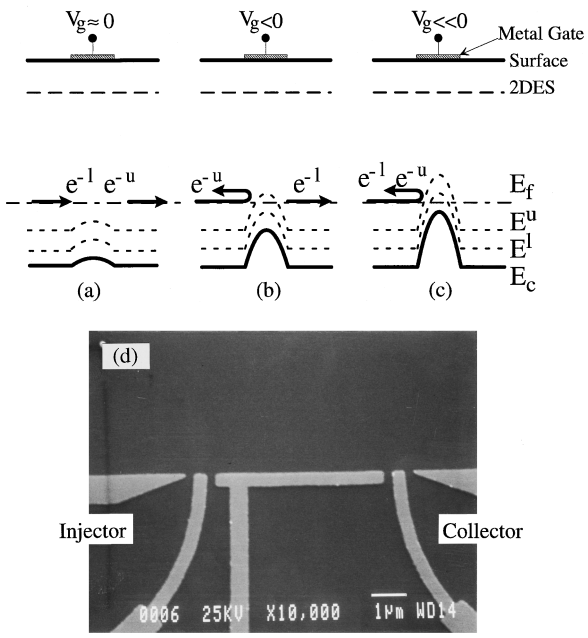

FIG. 2. Top figures (a)–(c) schematically illustrate the idea of using a tunable focusing barrier. The lower figure (d) shows a scanning electron micrograph of the device surface. The metal gates appear gray.

used to define injector and collector constrictions. These constrictions are 2000 Å wide and 6 μm apart.

All the measurements were made at 0.5 K using a standard low-frequency lock-in technique. We first made magnetotransport measurements with all the gates grounded (shorted to the 2DES). The measured Shubnikov–de Haas (SdH) oscillations are analyzed by determining the Fourier transform spectra of the resistance vs B^{-1} data. The subband densities thus obtained are 7.8×10^{10} cm^{-2} and 2.5×10^{11} cm^{-2}, the sum of which agrees with the total density obtained from the high field quantum Hall effect very well. The mobility of the 2DES is $\approx 2\times10^6$ cm^2/V s. The injector and collector constrictions were then defined by applying negative bias to the split gates (with respect to the 2DES) and monitoring the resistance of these constrictions via four-point probe measurements. Constrictions start to form when the split gates are biased at around -0.8 V and the point contact resistances are around 1.5 kΩ. During the TMF measurements, we made the constrictions smaller, with the point contact resistance for the injector ranging from 2 to 3 kΩ and the collector about 9 to 60 kΩ. Focusing spectra are measured by passing 100-nA current through the injector and detecting the collector voltage while sweeping B.

Figure 3 shows some typical focusing spectra, measured at fixed values of V_g applied to the focusing barrier surface gate with respect to the 2DES. Different curves are shifted vertically for clarity. The evolution discussed in Fig. 2 can be seen clearly in the data of Fig. 3. For the $V_g=0$ trace, the focusing spectrum shows only a single peak at $B=0.0275$ T, and is nearly featureless at higher B. The position of the single peak corresponds to the cyclotron orbit diameter of the LSE's matching L. As the barrier is raised by applying a negative V_g, the first focusing peak remains intact but new features, superimposed on a rising background, start to appear. For the smallest $V_g=-0.900$ V, when the focusing barrier is fully reflecting [Fig. 2(c)], strong oscillations whose frequency is consistent with the focusing of the LSE's are observed. In the intermediate range of barrier height, e.g., for $V_g=-0.275$ V, where we expect the focusing barrier to be transparent to the LSE's but reflective for the USE's, we observe weak oscillations which are periodic in B for $B\leqslant 0.1$ T. These oscillations, we believe, arise from the magnetic focusing of the USE's.

There are several reasons for this association: (1) The period of these oscillations and the positions of their peaks agree quite well with the expected values. The grid superimposed on the data in Fig. 3 shows the expected positions of the USE focusing peaks as deduced from the measured USE density using the SdH data.[8] (2) The gate voltage $V_g\approx -0.2$ V below which these oscillations start to appear matches the threshold voltage required to depopulate the USE's; this threshold voltage was measured in a different sample from the same wafer by depositing a uniform surface gate and monitoring the disappearance of the USE SdH oscillations. (3) As is well-known in TMF experiments, for sufficiently large B, when the cyclotron orbit diameter becomes comparable to the injector/collector constriction width, the focusing peaks are no longer observed. Note in Fig. 3 that we are able to observe the seventh peak for $V_g=-0.275$ V.[9] This is consistent with the focusing data at $V_g=-0.900$ V where six

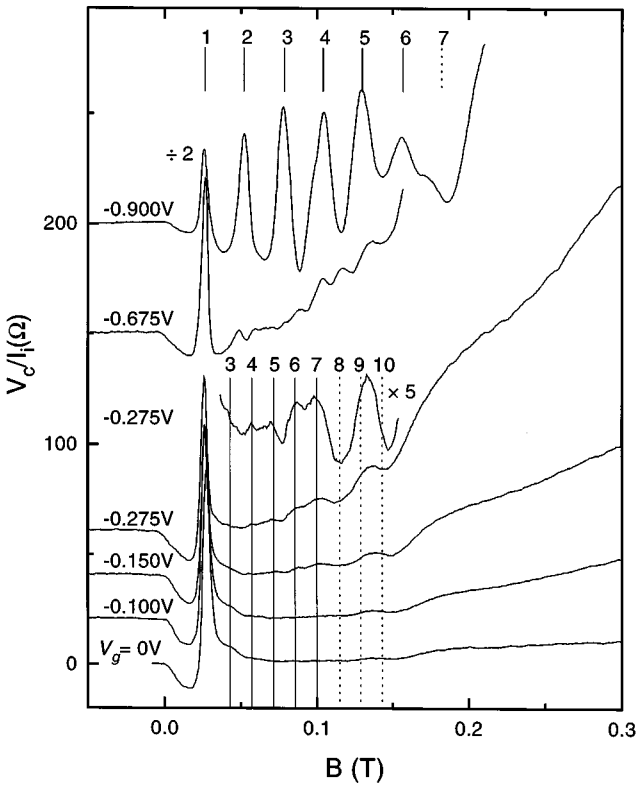

FIG. 3. Focusing spectra for different barrier heights. The vertical grids mark the positions of expected focusing peaks for the USE's (lower grid) and the LSE's (upper grid). The numbers denote the order of the expected focusing positions counted from $B=0$. For clarity, the $V_g=-0.275$ V data are shown amplified above the original trace; the amplified trace was obtained by subtracting a second-order polynomial background.

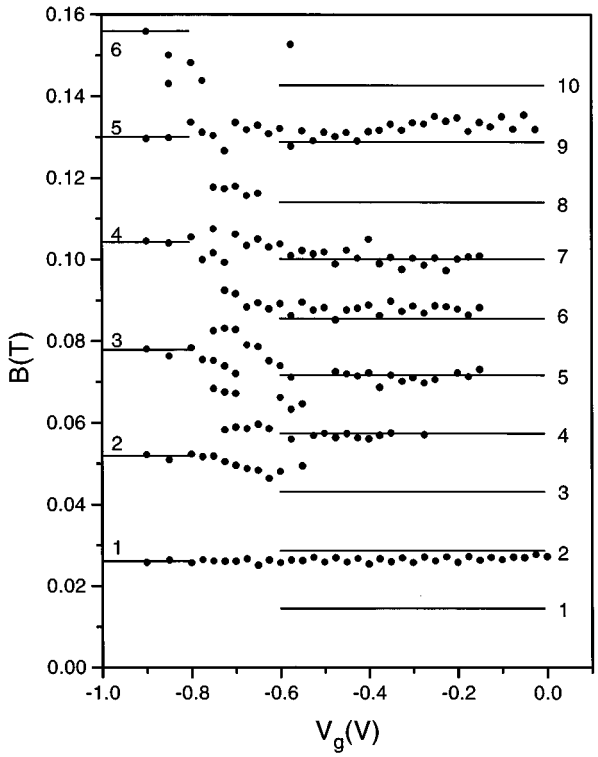

FIG. 4. Summary of the observed peak positions in the focusing spectra as a function of the focusing barrier gate bias. The horizontal grids mark the positions of the expected focusing peaks for the USE's (right-side grid) and the LSE's (left-side grid).

(possibly seven) peaks are observed for the LSE's: In both cases, when the orbit diameter becomes smaller than $L/6$ or $L/7$, the focusing signal disappears (the constriction is expected to be slightly narrower for the USE's). (4) The oscillations which we attribute to the USE focusing are reproducible in different cooldowns of the same sample. Moreover, via the application of a bias to a back gate which covers the entire back of the device, we were able to change the densities of electrons in both subbands. We observed shifts in the peak positions and oscillation frequency of the focusing spectra which are consistent with the changes in the subband densities. (5) Finally, on a similar device but with a focusing distance of $L=4$ μm we observe results which are consistent with the data of Fig. 3 and the shorter L. All these observations support our association of the weak maxima seen at intermediate V_g, where the USE's are selectively reflected, with the focusing of the ballistic USE's in this device.

In Fig. 4 we show a summary of the peak positions observed in the focusing spectra for $-0.9 \leqslant V_g \leqslant 0$ V. The evolution of the observed peak positions is clear. For $V_g \gtrsim -0.20$ V, a very strong peak corresponding to the main focusing peak of the LSE's is primarily observed. For $-0.55 \lesssim V_g \lesssim -0.20$ V, the USE focusing peaks are apparent, while for $V_g \lesssim -0.80$ V strong focusing peaks of the LSE's dominate. When $-0.55 \lesssim V_g \lesssim -0.8$ V, the focusing spectra are complicated (see Fig. 3 for $V_g=-0.675$ V) and show numerous peaks; this happens in the transition range where the focusing barrier is semitransparent for the LSE's.

The oscillations we observe at intermediate V_g and associate with the USE focusing effect are extremely weak compared to the LSE focusing peaks. This is consistent with the fact that we have never been able to observe the USE focusing signal in a standard TMF experiment. A possible explanation for this weakness may be that the ratio of the injected USE's to the LSE's is very small because the upper subband is depleted locally in the injector and collector openings. This explanation appears inadequate: First, in our standard TMF experiments, we are able to change the electron densities of both subbands as well as point-contact resistances of the injector and collector via a front gate covering the entire surface of the TMF device.[10] When a positive gate voltage of $+0.5$ V is applied, the electron densities are $\approx 1.5\times10^{11}$ cm^{-2} and 3×10^{11} cm^{-2} for USE and LSE, respectively, and point-contact resistances of injector and collector are both only ≈ 100 Ω. Under these conditions, the assumption that the upper subband is locally depleted in the injector and collector constrictions is unlikely and a comparable number of USE's and LSE's should pass through the openings. Yet we did not observe any trace of the USE focusing while the LSE's exhibit clear focusing. Second, in order to enhance the ratio of the number of injected USE's (relative to the LSE's), we raised the injection current in this device. Again, no USE focusing was observed. Finally, in our modified TMF experiment of Figs. 2–4, we tuned the opening widths of the injector and collector by changing the voltage applied to the split gates while always keeping the point-contact resistance of the injector below 3 kΩ to ensure that hot-electron effects are negligible. The best condition to observe the USE focus-

ing signal was achieved when the collector point-contact resistance (R_c) was larger than about 8 kΩ.[11] The reason for this best condition is not presently clear, but this observation certainly argues against the upper subband being locally depleted in the injector and collector constrictions.

A more plausible explanation for the weakness of the USE focusing signal is that the ballistic MFP for these electrons is very short. Since the amplitude of the focusing signal is proportional to $\exp(-L/l_f)$ where l_f is the (focusing) ballistic MFP,[7] this amplitude can be quite small if $l_f \ll L$. In order to estimate the USE ballistic MFP, we first measured the ballistic MFP of the LSE's in a separate, standard TMF device. This device, which was fabricated using material from the same wafer, had several focusing lengths. From the exponential decay plots of focusing amplitude vs L,[7] we were able to measure a LSE ballistic MFP of $l_f^l = 4.7$ μm. Using this value of l_f^l, and the ratio of the amplitudes of the USE and LSE focusing signals of Fig. 3 ($\approx$1%), we estimate a focusing ballistic MFP $l_f^u \approx 1$ μm for the USE's.

In Table I, we list several relevant parameters, namely, scattering times (τ) and MFP's for this two-subband system from different measurements. The values in the first row are deduced from the measured mobility by assuming that the two subbands have equal mobility. The second row shows the estimated values discussed in the last paragraph. The scattering times listed in the last row are obtained from the B dependence of the amplitude of the SdH oscillations.[12] To determine these amplitudes, the SdH oscillations of the two subbands were separated by inverse Fourier transforming the two frequency components. We then extract the scattering time τ by fitting the envelope of the SdH oscillations to an expression $\propto \exp(-\pi/\omega_c \tau)$, where ω_c is the cyclotron frequency. It is clear from Table I that the MFP's estimated from the mobility are almost 100 times larger than those deduced from the SdH oscillations, while the values estimated from the focusing experiments fall in between. This is similar to what is observed in single-subband 2DES (Ref. 13) and is not very surprising since, e.g., small-angle scattering plays a much more important role in limiting the SdH scattering time than the mobility scattering time.[14] However, it is surprising that the l_f^u estimated from the focusing experiments is almost five times smaller than l_f^l while l^u is only 30% shorter than l^l in SdH measurements. It is unlikely that intersubband scattering is responsible for this observation: although such a scattering mechanism may be operative in a two-subband system,[15] it should equally affect both subbands and cannot explain the much shorter l_f^u. A possible explanation may be that the USE's, having a smaller k_f, are scattered at a larger angle for a given scattering wave vector. Another possibility is that the USE's suffer more interface roughness scattering. We do not have an independent confirmation of these hypotheses at present, and plan on future studies.

TABLE I. Scattering times (τ) and mean free paths (l) of the two-subband system from different measurements.

	τ^l (ps)	τ^u (ps)	l^l (μm)	l^u (μm)
Mobility	(85)	(85)	(18)	(10)
Focusing	24	8.3	4.7	1
SdH	1.0	1.3	0.22	0.16

In summary, we use a specially designed magnetic focusing experiment to study the upper-subband ballistic electrons in a wide, square quantum well. The much weaker focusing signal of the USE's compared to that of the LSE's implies a surprisingly short USE ballistic MFP.

We thank M. B. Santos for sample growth. This work was supported by the Army Research Office and the National Science Foundation.

[1] See, e.g., Y. W. Suen, H. C. Manoharan, X. Ying, M. B. Santos, and M. Shayegan, Phys. Rev. Lett. **72**, 3405 (1994), and references therein.

[2] B. Laikhtman, U. Sivan, A. Yacoby, C. P. Umbach, M. Heiblum, J. A. Kash, and H. Shtrikman, Phys. Rev. Lett. **65**, 2181 (1990).

[3] R. I. Hornsey, J. R. A. Cleaver, and H. Ahmed, Phys. Rev. B **48**, 14 679 (1993).

[4] J. P. Lu and M. Shayegan (unpublished).

[5] V. S. Tsoi, Pis'ma Zh. Eksp. Teor. Fiz. **19**, 114 (1974) [JETP Lett. **19**, 70 (1974)].

[6] H. van Houten *et al.*, Phys. Rev. B **39**, 8556 (1989).

[7] J. Spector, H. L. Stormer, K. W. Baldwin, L. N. Pfeiffer, and K. W. West, Surf. Sci. **228**, 283 (1990).

[8] The periods of the grids shown in Figs. 3 and 4 for the USE's and LSE's are $\approx$6% and 5% lower than the values deduced from the measured USE and LSE densities, respectively. This discrepancy, however, is well within our experimental accuracy.

[9] The eighth peak is clearly missing in Fig. 3; the peak observed between the ninth and tenth expected focusing peaks must have a different origin since its position is wrong and it also shows up in all the focusing spectra, including the one with $V_g = 0$.

[10] The injector and collector constrictions and the focusing barrier for this device were defined by a deep etching prior to depositing the metal front gate.

[11] When $R_c \lesssim 8$ kΩ, we observed essentially no focusing signal except for the single peak at $B = 0.0275$ T for $-0.55 \lesssim V_g \lesssim 0$ V and, for $-0.8 \lesssim V_g \lesssim -0.55$ V, peaks whose positions smoothly shift with V_g. The dependence of these peaks' positions on V_g is consistent with the barrier selectively reflecting LSE's impinging on it at an angle and with a kinetic energy perpendicular to the barrier which is smaller than the barrier height. We do not observe such angular effect when $R_c \gtrsim 8$ kΩ, probably because of the narrow acceptance angle of the collector point contact.

[12] T. Ando, J. Phys. Soc. Jpn. **37**, 1233 (1974).

[13] J. J. Heremans and M. Shayegan (unpublished).

[14] S. Das Sarma and F. Stern, Phys. Rev. B **32**, 8442 (1985).

[15] See, e.g., T. P. Smith III, F. F. Fang, U. Meirav, and M. Heiblum, Phys. Rev. B **38**, 12 744 (1988); R. Fletcher, E. Zaremba, M. D'Iorio, C. T. Foxon, and J. J. Harris, *ibid.* **38**, 7866 (1988).